

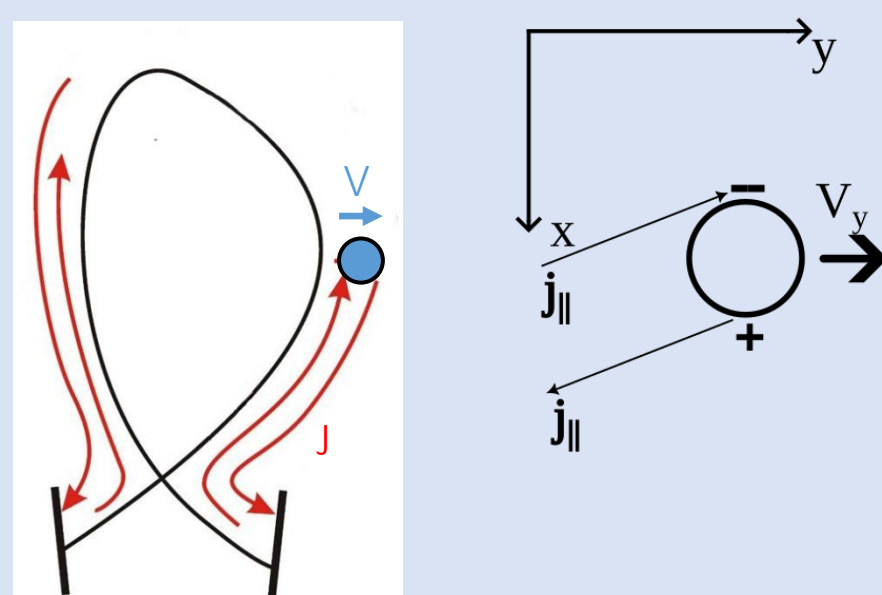
INTRODUCTION

- One of the key problems for tokamak-reactor - sputtering of plasma facing components - takes greater significance as a result of the recent ITER re-baselining in which the beryllium main chamber armour has been replaced by tungsten (W) [1].
- Choice of the reactor scenario is based on the boundary plasma modeling (SOLPS-ITER, SOLEDGE3X etc.)
- Until recently, the SOLPS simulation domain has been restricted to an area in the SOL limited by a last flux surface which connects the two divertor targets and just avoids intersecting the main chamber walls.
- In the last few years a wide unstructured grid approach has been developed [2], so that plasma simulations can be performed up to the real surfaces.
- Here, the first modeling of ITER burning plasmas, including neon seeding for divertor power flux control, with the new SOLPS-ITER 3.2.0 code version featuring a wide-grid capability is presented.
- The primary objectives of the study is more realistic description of the plasma flows onto the wall, and the production of simulated plasma backgrounds which can later be used by other codes for the study of tungsten sputtering and migration.
- For the first time for such a scenario convergence of SOLPS-ITER 3.2.0 was achieved with the equation for the electrostatic potential included in the calculations.
- The transport coefficient scan is performed around the values based on the estimates, which are made assuming filamentary transport in the far SOL

ESTIMATES FOR FAR SOL TRANSPORT COEFFICIENTS

Assumptions based on both modeling and experimental observations [3]:

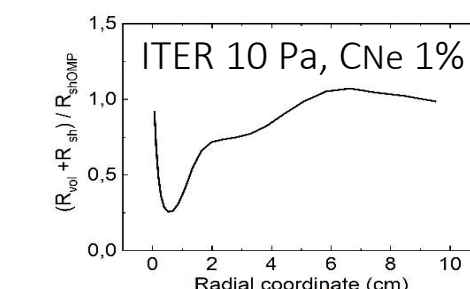
- SOL plasma transport with the sequence of individual filaments.
- Filaments of some typical most stable dimensions follow each after the other, without big time delay.
- Filaments are electrically connected to the divertor targets; based on the observation that in low collisionality case the filaments of a size corresponding to beginning of their electric disconnection are mainly observed.
- Filament radial propagation length is of the same order as its initial size l_{\perp} .



Radial filament velocity $V_y = \frac{2\delta n(T_e + T_i)T_e l_{\parallel}}{nc_s e^2 B^2 R l_{\perp}^2} \frac{R_{vol} + R_{sh}}{R_{shOMP}}$ is determined by $\vec{E} \times \vec{B}$ drift caused by its polarization by ∇B -driven current. Density perturbation: $\delta n = l_{\perp} \frac{\partial n}{\partial r} = l_{\perp} \frac{n}{\lambda_n}$. The average radial flow associated with filaments doesn't depend on their typical size $\langle \delta n V_y \rangle = \frac{2n(T_e + T_i)T_e l_{\parallel}}{c_s e^2 B^2 R \lambda_n^2} \frac{R_{vol} + R_{sh}}{R_{shOMP}}$.

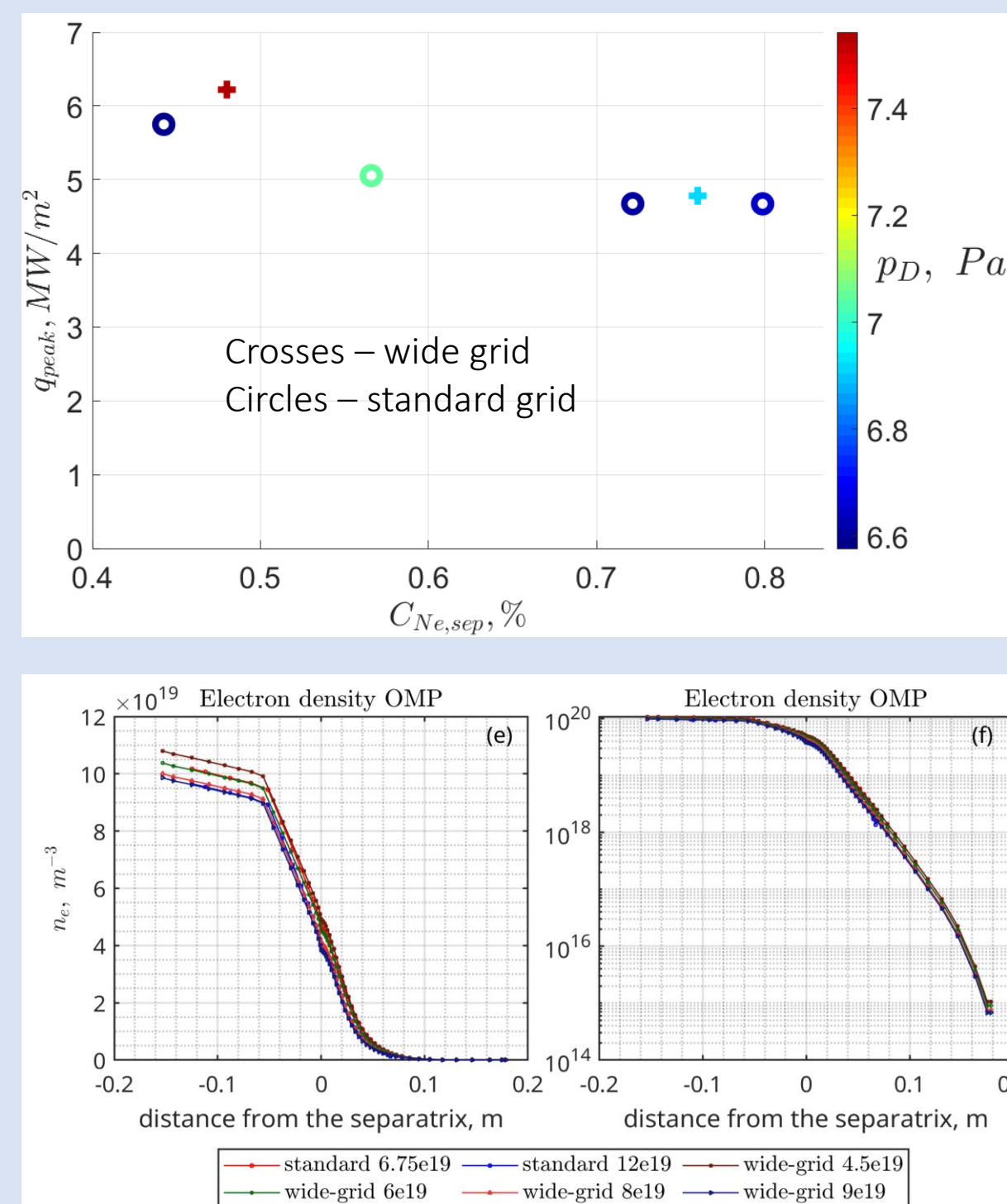
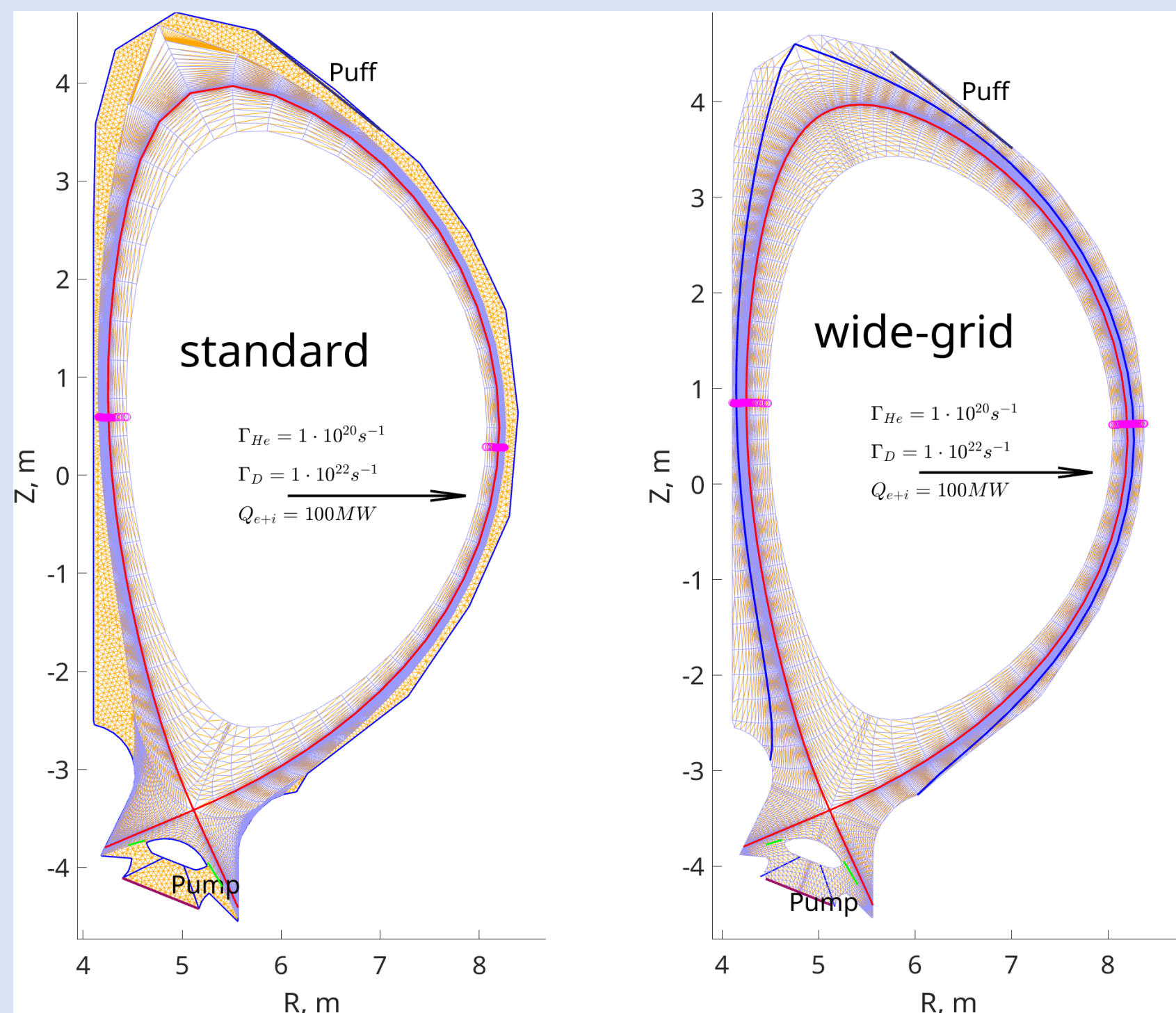
SOL radial scale for density: $\frac{\langle \delta n V_y \rangle}{\lambda_n} \approx \frac{nc_s}{l_{\parallel}} \rightarrow \lambda_n \approx \left(\frac{2(T_e + T_i)T_e l_{\parallel}^2}{e^2 B^2 R c_s^2} \frac{R_{vol} + R_{sh}}{R_{shOMP}} \right)^{1/3}$

Diffusion coefficient: $Dn/\lambda_n^2 \approx nc_s/l_{\parallel} \rightarrow D = \left(\frac{T_{eOMP}}{e} \right)^{4/3} B^{-4/3} \left(1 + \frac{T_{iOMP}}{T_{eOMP}} \right)^{2/3} \left(\frac{4r}{R^2 b_x c_s} \right)^{1/3} \left(\frac{R_{vol} + R_{sh}}{R_{shOMP}} \right)^{2/3}$



Modeling setup. Benchmarking with standard SOLPS-ITER modeling

- Anomalous diffusion coefficient $D_{AN, farSOL} = 0.3 \text{ m}^2/\text{s}$
- D puffing $5 \cdot 10^{22} \text{ at} \cdot \text{s}^{-1}$
- Ne seeding $6.75 - 12 \cdot 10^{19} \text{ at} \cdot \text{s}^{-1}$ for the standard grid and $4.5 - 9 \cdot 10^{19} \text{ at} \cdot \text{s}^{-1}$ for the wide grid case.
- Pumping coefficient is set by a feedback scheme to achieve D atom and molecule pressure in PFR $p_D = 7 \text{ Pa}$.
- Input power equally shared between electrons and ions $P_{e+i} = 100 \text{ MW}$.
- Magnetic equilibrium and wall contour from shot IMAS #116000, run#4.
- Distance between primary and secondary separatrices at the OMP of $\sim 6.5 \text{ cm}$, $B_t = 5.3 \text{ T}$, $I_p = 15 \text{ MA}$.
- Current continuity equation is solved, but the drift terms are put zero.



CONCLUSION

- The SOLPS-ITER 3.2.0 results were compared with those from SOLPS-ITER 3.0.8 simulations performed on the standard narrower grid which has hitherto dominated all SOLPS studies for ITER. The comparison was performed for constant moderate SOL transport level, previously typically used for ITER modeling. In the common computational domain both the wide and narrow grid codes yield closely similar results.
- In a subsequent study, focusing only on the wide-grid simulations, the cross-field transport coefficients in the far-SOL were increased in order to simulate the possible widening of SOL (the so-called shoulder formation) due to increased convective (filamentary) transport. The typical effective diffusivity values in the SOL region of filamentary transport, used in the modeling, are based on the presented simple but robust model estimates. The transport parameters were varied over a wide range around the values expected from estimates as well as the distance from separatrix where the filamentary transport starts to dominate and the transport needs to be increased.
- In the limiting case of factor 30 the characteristic density scale length in the far-SOL has increased approximately by factor of 3. The electron temperature decreases at scales comparable to those of density, while the ion temperature decreases considerably more slowly. The ion temperature decay length can exceed 10 cm, leading to high (of the order of several tens of eV) ion temperature at the wall.
- An increase of the diffusion coefficient up to values $D_{AN, farSOL} \geq 5 \text{ m}^2/\text{s}$ leads to an increase of the ionization source inside the separatrix. For lower values of the diffusion coefficient, obtained from estimates based on simple models of filamentary transport and for modeling of semi-detached regimes of modern tokamaks, the far-SOL transport does not significantly affect the plasma parameters inside the separatrix.
- The flow of main ions and seeded impurity to the wall at the outer and inner midplanes increases by approximately two orders of magnitude when the diffusion coefficient increases from $D_{AN, farSOL} = 0.3 \text{ m}^2/\text{s}$ to $D_{AN, farSOL} = 2 \text{ m}^2/\text{s}$. The latter value can be taken as a reasonably pessimistic scenario.

Transport coefficient scan in wide grid modeling

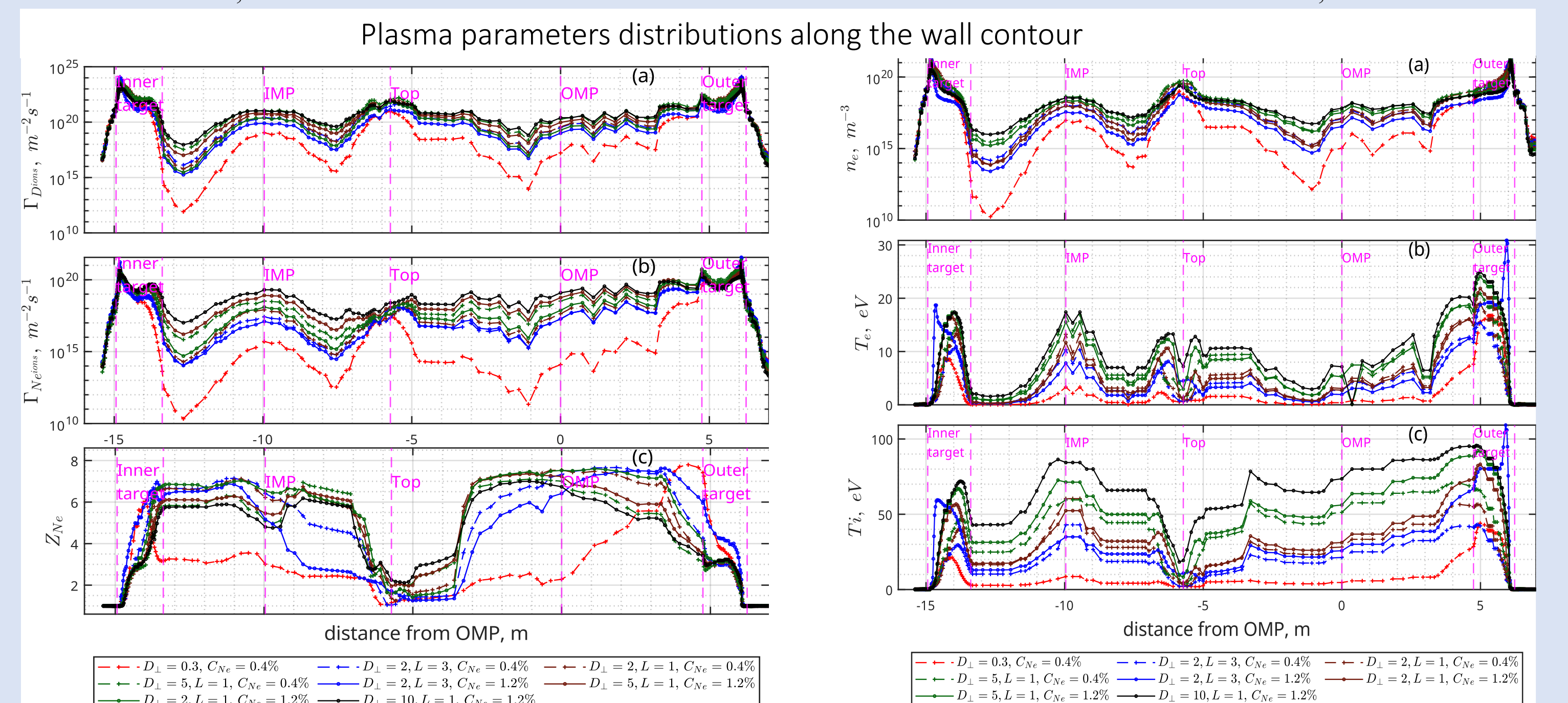
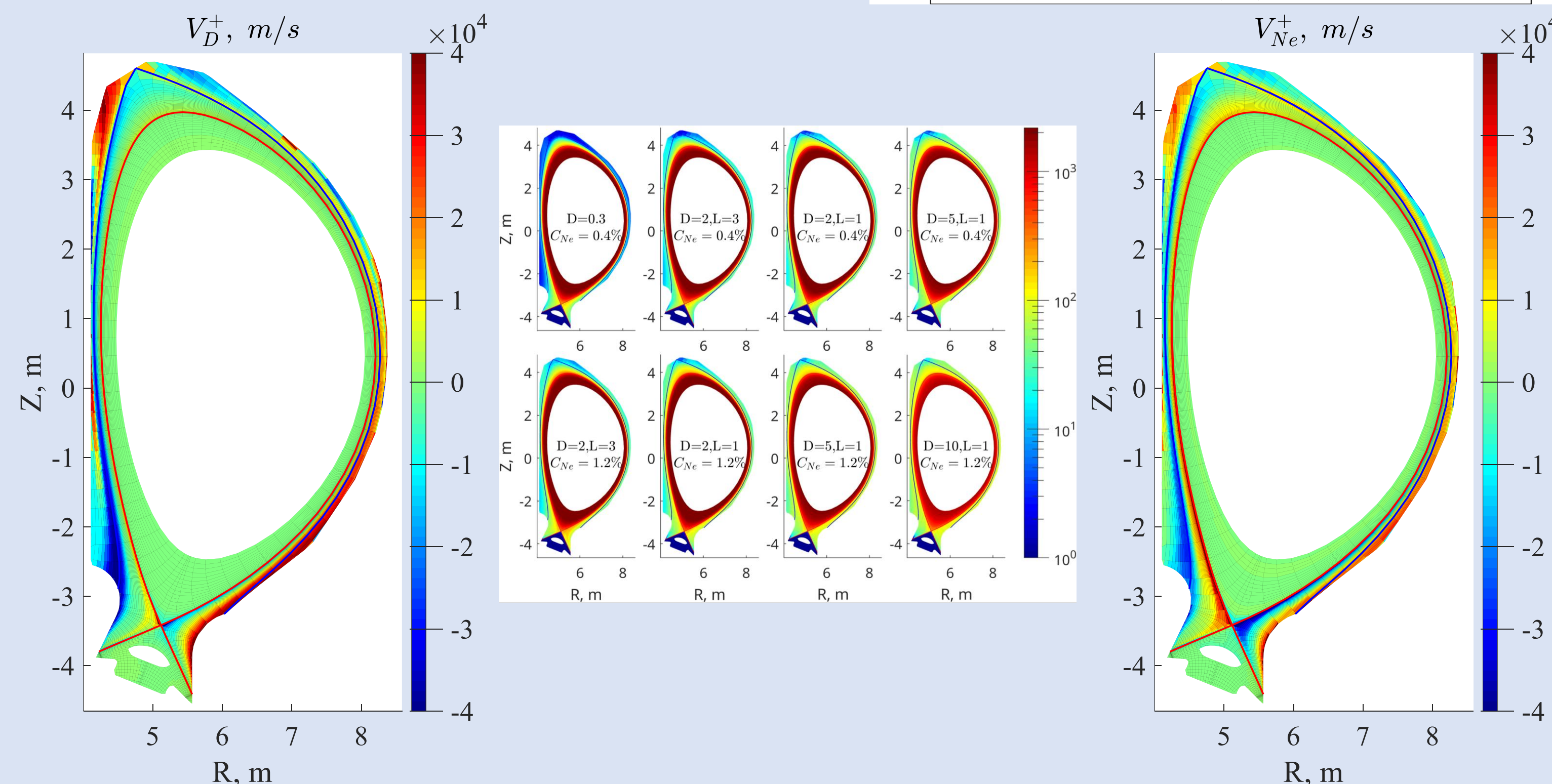
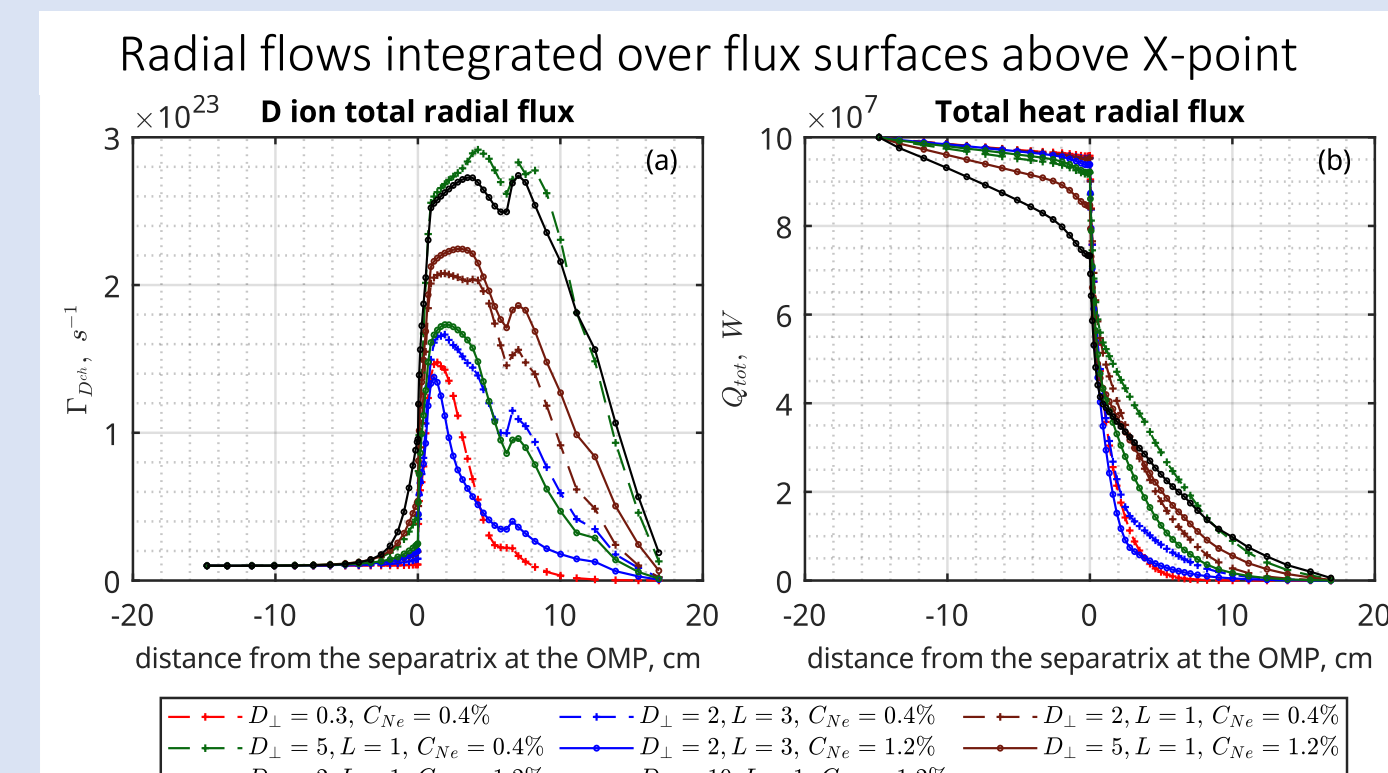
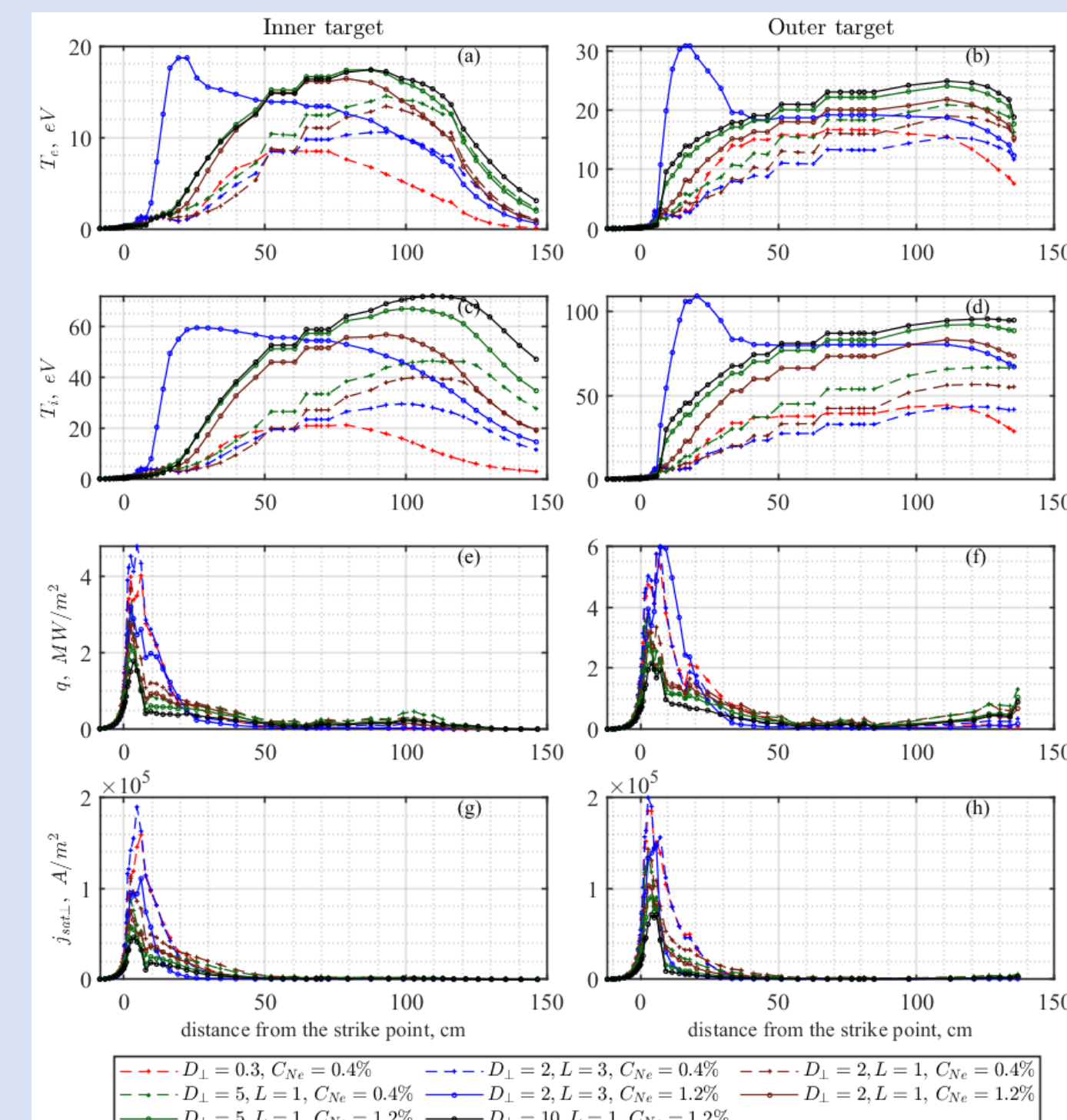
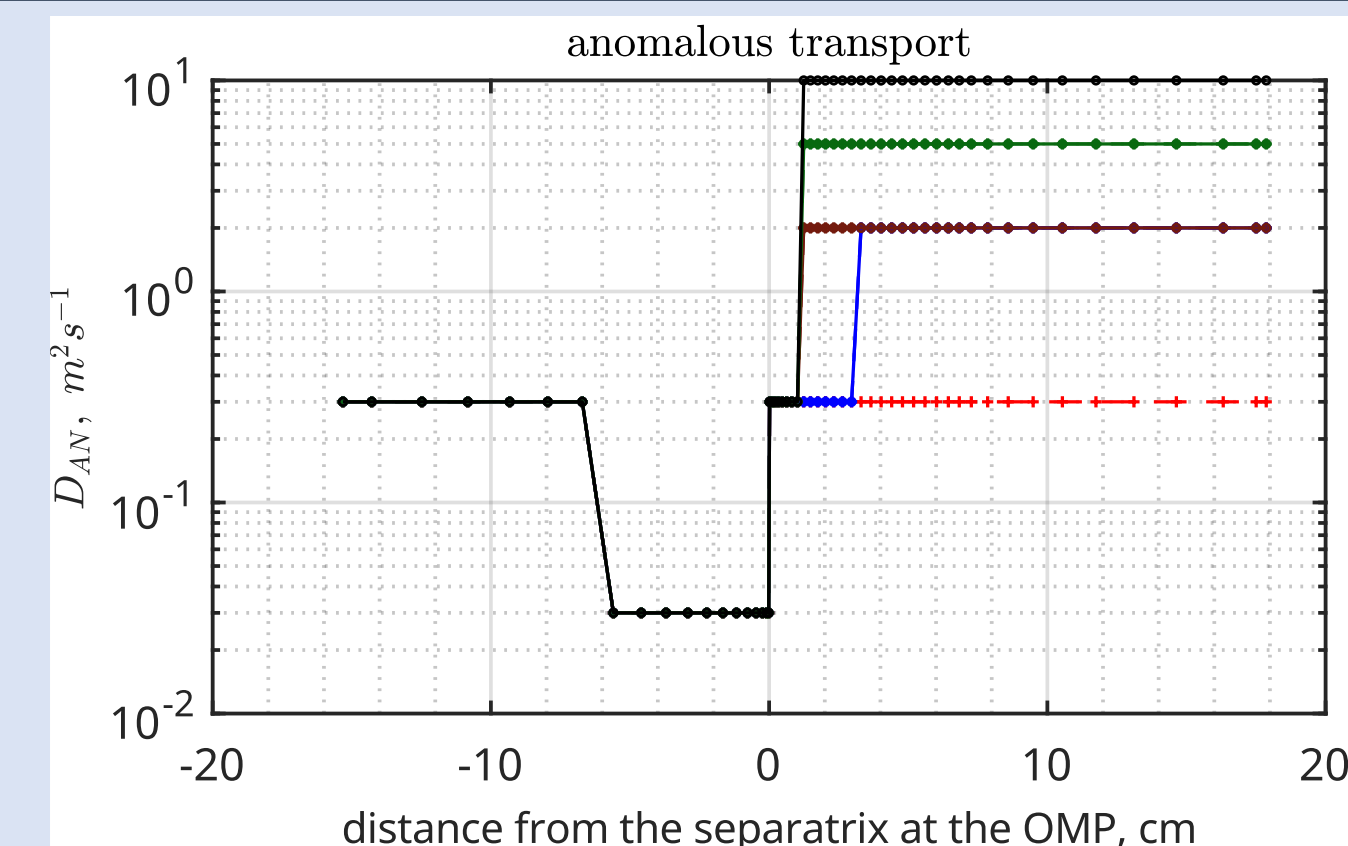
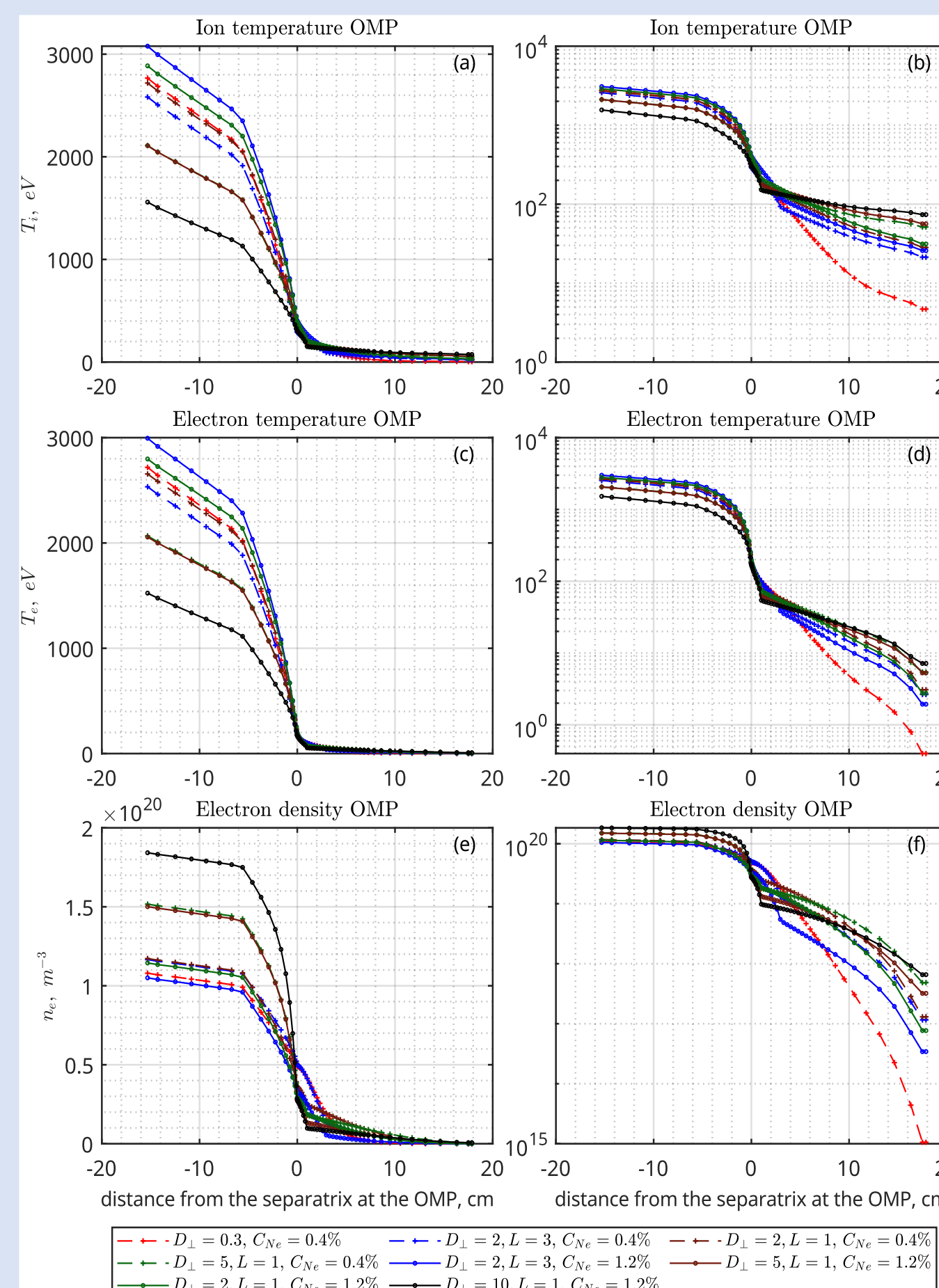
	$C_{Ne}, \%$	$\lambda_{Te}, \text{ cm}$	$\lambda_{Ti}, \text{ cm}$	$\lambda_n, \text{ cm}$
D=0.3	0.4	3.7	7.8	1.7
D=2, L=3	0.4	5.3	13.1	2.9
D=2, L=1	0.4	5	12.5	2.7
D=5, L=1	0.4	5.8	22.5	3.6
D=2, L=3	1.2	5.2	12.9	2.9
D=2, L=1	1.2	5	12.2	2.7
D=5, L=1	1.2	6.1	20.4	3.6
D=10, L=1	1.2	6.8	35.3	4.8

$$\lambda_{Te}/\lambda_n > 1, \quad \lambda_{Ti}/\lambda_n > 1$$

Can be explained by simple balance:

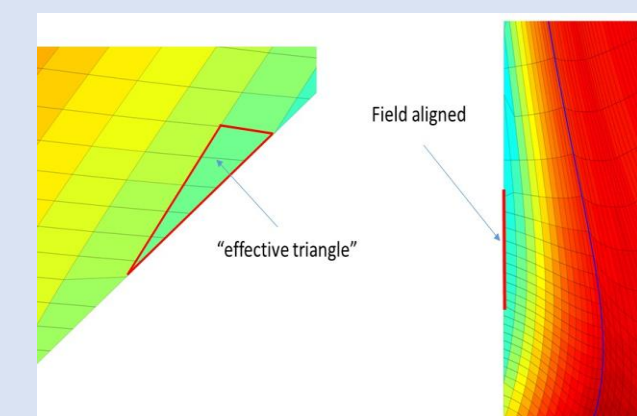
$$\nabla \cdot \left(\frac{3}{2} n T_{e,i} (\vec{V}_{diff} + \vec{V}_{||}) + \vec{q} \right) = -n T_{e,i} \nabla \cdot \vec{V}_{||}$$

with account of corresponding sheath transmission factors

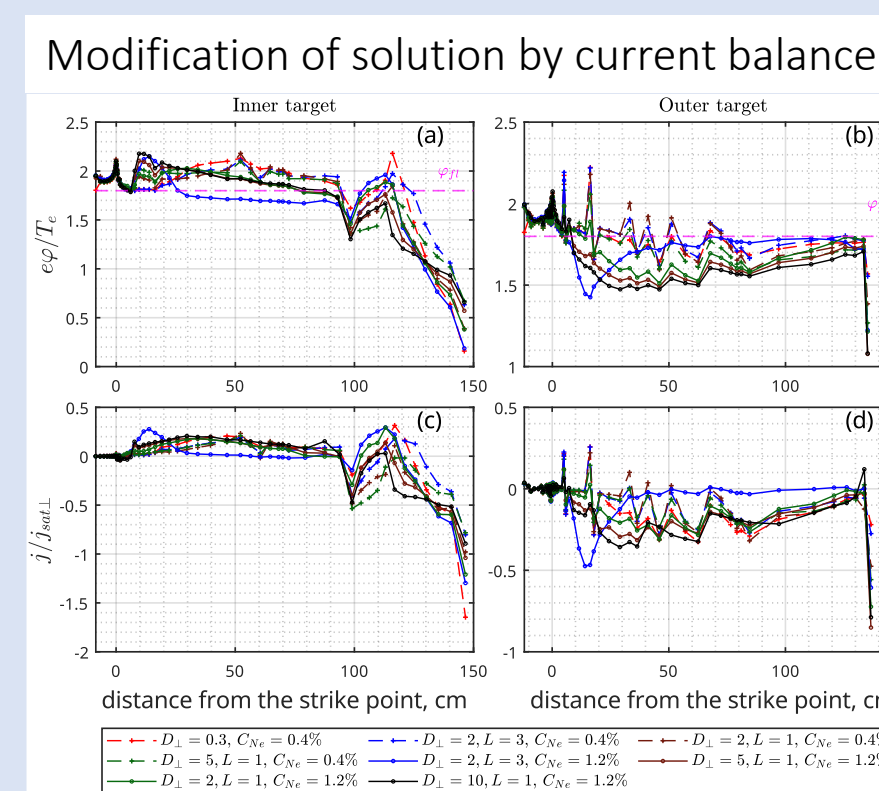


Technical issues

- Boundary conditions:
 - separation of field aligned and non-field aligned boundaries
 - treatment of non-field aligned sequence of trapezoidal and triangular cell faces at the ends of flux tubes
- Correction of energy transport by turbulent convection
- Modification of flux limiting and heat sources in low collisionality far-SOL regions



$$\tilde{k}_{||} \approx k_{||} \frac{1}{1 + \left(c_{f1} \int_{wall1}^{wall2} V_{||} \frac{dl}{c_s} \right)^{-1}}$$



ACKNOWLEDGEMENTS / REFERENCES

This work was supported by the ITER International Fusion Energy Organization Service Contract No. IO/23/CT/4300002968 of 24.11.2023. This work was performed under the auspices of the ITER Scientist Fellow Network. The views and opinions expressed herein do not necessarily reflect those of the ITER Organization. Numerical calculations were performed at the Polytechnic Supercomputer Center at Peter the Great St. Petersburg Polytechnic University

- PITTS, R. A. et al., Plasma-wall interaction impact of the ITER re-baseline, Nucl. Mater. Energy **42** (2025) 101854
- DEKEYSER, W. et al., Plasma edge simulations including realistic wall geometry with SOLPS-ITER, Nucl. Mater. Energy **27** (2021) 100999
- D'IPPOLITO, D.A., MYRA, J.R., ZWEBEN, S.J. Convective transport by intermittent blob-filaments: Comparison of theory and experiment, Phys. Plasmas **18** (2011) 060501